

New Fused Heteroarenes for High-Performance Field-Effect TransistorsJie-Yu Wang,[†] Yan Zhou,^{†,‡} Jing Yan,[†] Lin Ding,[†]
Yuguo Ma,^{*,†} Yong Cao,[‡] Jian Wang,^{*,‡} and Jian Pei^{*,†}

[†]The Key Laboratories of Bioorganic Chemistry and Molecular Engineering and of Polymer Chemistry and Physics of Ministry of Education, College of Chemistry and Molecular Engineering, Peking University, Beijing 100871, and [‡]Institute of Polymer Optoelectronic Materials and Devices, South China University of Technology, the Key Laboratory of Specially Functional Materials of Ministry of Education, Guangzhou 510640, China

Received February 26, 2009

Revised Manuscript Received April 29, 2009

Recently, many planar organic conjugated materials have been developed for next-generation electronic devices, such as field-effect transistors (FET).¹ Among them, oligoarenes fused with thiophene units were demonstrated to possess remarkable performance and high stability in FET.² In our previous contributions, several new types of semiconductors based on the benzothiophene unit were synthesized and exhibited good FET performance with high stability in air.³ Devices from a fused arene with an anthracene core showed mobility up to $0.01 \text{ cm}^2 \text{ V}^{-1} \text{ s}^{-1}$.⁴ To develop new soluble and stable organic materials for FET devices via a simple solution process and to further investigate the relationship between molecular structures and device performance, in this contribution, we design a new skeleton with a chrysene core for active materials in FET. Such an extension not only enlarges the conjugated plane but also changes the overall symmetry of the molecule, which might have properties different from that of much explored linear acenes.⁵ Top-contact FET devices using **1a** and **1b** as the active materials show high hole mobility up to $0.4 \text{ cm}^2 \text{ V}^{-1} \text{ s}^{-1}$.

Figure 1 shows the molecular structure of our newly designed materials, which shares a chrysene-based, thiophene-containing

heteroarene core. We first carried out geometry optimization on their core structure with DFT(B3LYP) method on 6-31G(d) level.⁶ From the side view of the optimized core structure, a significant twist (with a dihedral angle of about 15°) in the central part of the conjugated system was observed, caused by the repulsion between the sulfur atom and the hydrogen atom on the naphthalene skeleton.

Scheme 1 illustrates the synthetic approach to **1a** and **1b**. Bromination of a commercially available material **2** with NBS followed by demethylation with BBr_3 in CH_2Cl_2 afforded **4** in nearly quantitative yield.⁷ Compound **4** reacted with trifluoromethanesulfonic anhydride to afford compound **5** in 56% yield. A Negishi cross-coupling reaction between **5** and 5-alkyl-2-thienylzinc chloride, which was prepared in situ from lithiation of 2-alkylthiophene with *n*-BuLi followed by addition of anhydrous zinc chloride, produced **6a** and **6b** in about 90% yield. Finally, oxidative cyclization of **6a** and **6b** using ferric chloride in CH_2Cl_2 gave target molecules **1a** and **1b** in around 80% yield, respectively. **1a** and **1b** dissolved well in common organic solvents, such as CHCl_3 and toluene. The structures and purity of both **1a** and **1b** were confirmed by ^1H and ^{13}C NMR spectroscopy, EI-MS, and elemental analysis (see the Supporting Information). The thermal decomposition temperature of **1a** and **1b** under a nitrogen atmosphere was around 400°C , indicating their good thermal stability. The HOMO energy levels in thin film were calculated from the onset of oxidation waves in the cyclic voltammetry to be -5.35 eV for both **1a** and **1b**. The relatively low HOMO levels and large band gap, compared with tetracene derivatives,⁸ were caused by the phenanthrene-like connectivity of the central chrysene core.

To test whether these molecules could be used as active materials in FET, top-contact FET devices were fabricated. A thin film of **1a** with a thickness of 40 nm as the active layer was deposited on an OTS (octadecyltrichlorosilane)-treated SiO_2 (300 nm)/Si substrate at $4 \times 10^{-4} \text{ Pa}$. Gold was then deposited by thermal evaporation at $4 \times 10^{-4} \text{ Pa}$ as the electrode. Thin film transistor characteristics of **1a** were measured under an ambient atmosphere on 15 devices, all of which performed as p-channel transistors with hole mobility ranging between 0.1 and $0.4 \text{ cm}^2 \text{ V}^{-1} \text{ s}^{-1}$ and an on/off ratio of about 1×10^4 . Figure 2 illustrates transfer and output characteristics of **1a** in OFET. We also varied the substrate temperature during vacuum deposition, and the best results were obtained by keeping the substrate at room temperature. All devices showed good stability: the device performances did not drop significantly

*Corresponding author. E-mail: jianpei@pku.edu.cn.

- (1) (a) Allard, S.; Forster, M.; Souharce, B.; Thiem, H.; Scherf, U. *Angew. Chem., Int. Ed.* **2008**, *47*, 4070. (b) Dimitrakopoulos, C. D.; Malenfant, P. R. L. *Adv. Mater.* **2002**, *14*, 99. (c) Ahmed, E.; Briseno, A. L.; Xia, Y.; Jenekhe, S. A. *J. Am. Chem. Soc.* **2008**, *130*, 1118. (d) Lim, J. A.; Lee, H. S.; Lee, W. H.; Cho, K. *Adv. Funct. Mater.* **2008**, ASAP.
- (2) (a) Takimiya, K.; Ebata, H.; Sakamoto, K.; Izawa, T.; Otsubo, T.; Kunugi, Y. *J. Am. Chem. Soc.* **2006**, *128*, 12604. (b) Yamamoto, T.; Takimiya, K. *J. Am. Chem. Soc.* **2007**, *129*, 2224. (c) Xiao, K.; Liu, Y.; Qi, T.; Zhang, W.; Wang, F.; Gao, J.; Qiu, W.; Ma, Y.; Cui, G.; Chen, S.; Zhan, X.; Yu, G.; Qin, J.; Hu, W.; Zhu, D. *J. Am. Chem. Soc.* **2005**, *127*, 13281. (d) Sakamoto, M.; Tachikawa, T.; Fujitsuka, M.; Majima, T. *Chem. Mater.* **2008**, *20*, 2060.
- (3) Zhou, Y.; Liu, W.-J.; Ma, Y.; Wang, H.; Qi, L.; Cao, Y.; Wang, J.; Pei, J. *J. Am. Chem. Soc.* **2007**, *129*, 12386.
- (4) Liu, W.-J.; Zhou, Y.; Ma, Y.; Cao, Y.; Wang, J.; Pei, J. *Org. Lett.* **2007**, *9*, 4187.
- (5) (a) Anthony, J. E. *Angew. Chem., Int. Ed.* **2008**, *47*, 452. (b) Okamoto, H.; Kawasaki, N.; Kaji, Y.; Kubozono, Y.; Fujiwara, A.; Yamaji, M. *J. Am. Chem. Soc.* **2008**, *130*, 10470.

- (6) Frisch, M. J.; et al. Gaussian 03, revision B.05; Gaussian, Inc.: Pittsburgh, PA, 2003.
- (7) Chakravart, S. N.; Pasupati, V. *J. Chem. Soc.* **1937**, 1859.
- (8) (a) Ionkin, A. S.; Marshall, W. J.; Fish, B. M.; Bryman, L. M.; Wang, Y. *Chem. Commun.* **2008**, 2319. (b) Odom, S. A.; Parkin, S. R.; Anthony, J. E. *Org. Lett.* **2003**, *5*, 4245.

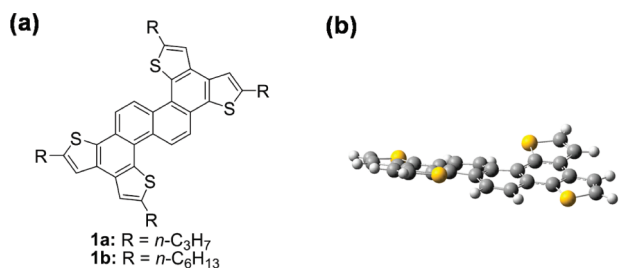
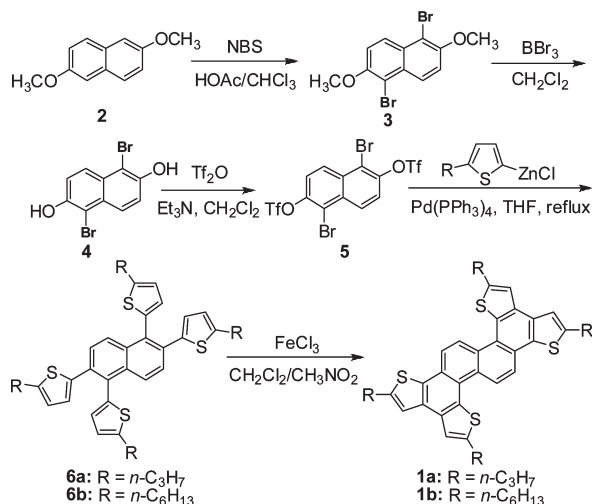


Figure 1. (a) Molecular structure of **1a** and **1b**. (b) Optimized core structure.

Scheme 1. Synthetic Approach to **1a** and **1b**



for at least one month storage under ambient condition with 70% humidity. Such a high performance was unexpected, considering the moderate mobility of their smaller planar analogues with one less benzene ring.⁹

To understand the origin of the high mobility, we first attempted to elucidate the structure of **1a** in the solid state. Single crystals suitable for X-ray analysis were grown by slowly evaporating a dilute solution of **1a** in 1,4-dioxane. The crystal assumed a “layer-by-layer” structure with alternating alkyl chains and arene cores. In addition, significant S–S contact was observed in the plane normal to the stacking direction (as shown in Figure 3b), which provided another conductive channel inside the layer.¹⁰ The central arene adopted an almost flat configuration in solid state (with a dihedral angle of ca. 3.2°), which can be clearly seen from its side view (Figure 3a). This result is in great contrast to the conformation of the molecule in vacuum. Calculation on this core conformation shows that it is not a local minimum; it relaxes into a conformation with a

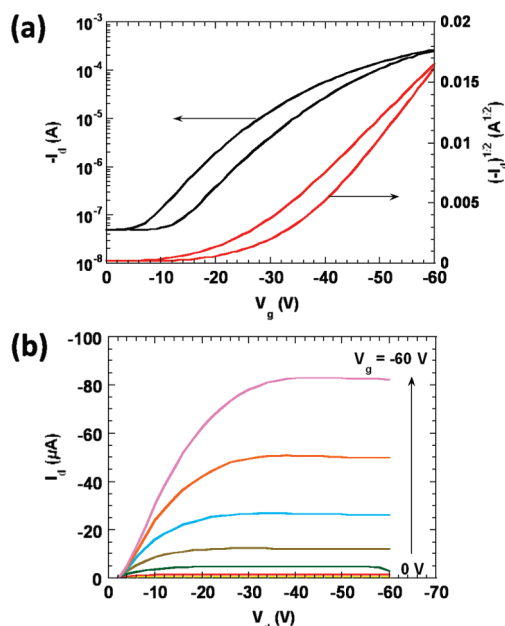


Figure 2. Electrical characteristics of the OFET for **1a**: (a) transfer characteristic, (b) output characteristic.

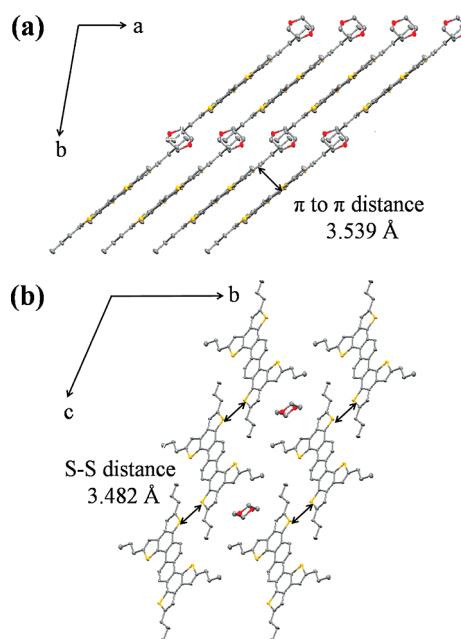


Figure 3. Single-crystal structure of **1a** (a) viewed along the *c* axis and (b) viewed along the *a* axis. Solvent molecules were included in the crystal.

dihedral angle of 6.7°, which still lies 0.91 kcal mol^{−1} higher than the structure with a larger twist. We supposed that the strong intermolecular interaction, particularly π – π stacking (the distance between two adjacent arenes is 3.5 Å), forced the molecules to take a much flatter shape than in gas phase. In other words, favorable intermolecular π – π stacking in the flat conformation overcomes the intramolecular repulsion between the lone pair electrons of sulfur atom and hydrogen. Such planarization provides the explanation for the observed high OFET performance of **1a**. Calculation on the reorganization energy of the optimized structure and the single-crystal structure shows that the one in the solid state has slightly lower reorganization energy

- (9) Brusso, J. L.; Hirst, O. D.; Dadvand, A.; Ganesan, S.; Cicoira, F.; Robertson, C. M.; Oakley, R. T.; Rosei, F.; Perepichka, D. F. *Chem. Mater.* **2008**, *20*, 2484.
- (10) (a) Sun, Y.; Tan, L.; Jiang, S.; Qian, H.; Wang, Z.; Yan, D.; Di, C.; Wang, Y.; Wu, W.; Yu, G.; Yan, S.; Wang, C.; Hu, W.; Liu, Y.; Zhu, D. *J. Am. Chem. Soc.* **2007**, *129*, 1882. (b) Ebata, H.; Izawa, T.; Miyazaki, E.; Takimiya, K.; Ikeda, M.; Kuwabara, H.; Yui, T. *J. Am. Chem. Soc.* **2007**, *129*, 15732. (c) Briseno, A. L.; Miao, Q.; Ling, M.-M.; Reese, C.; Meng, H.; Bao, Z.; Wudl, F. *J. Am. Chem. Soc.* **2006**, *128*, 15576. (d) Dadvand, A.; Cicoira, F.; Chernichenko, K. Y.; Balenkova, E. S.; Osuna, R. M.; Rosei, F.; Nenajdenko, V. G.; Perepichka, D. F. *Chem. Commun.* **2008**, 5354.

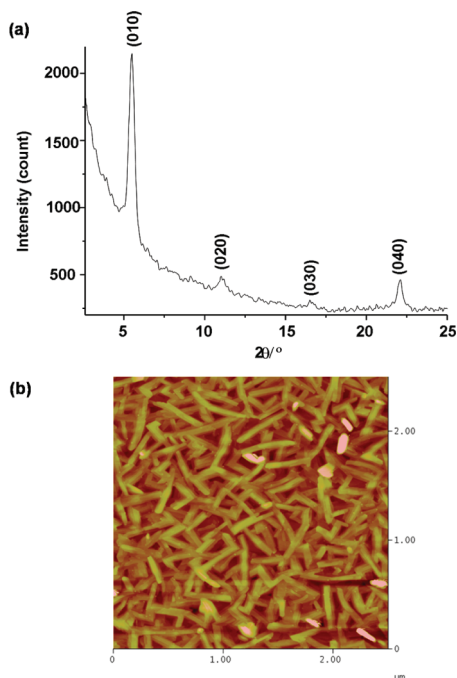


Figure 4. Thin film characterization. (a) X-ray reflection diagram of **1a** thin film deposited on OTS-treated Si/SiO₂ substrate at room temperature. (b) Corresponding AFM image (2.5 μm × 2.5 μm).

(3.75 kcal/mol for the flat configuration and 4.02 kcal/mol for the twisted configuration), which is an important factor in determining the charge transporting ability of a material.¹¹

We then characterized the thin film structure by X-ray diffraction and atomic force microscopy (AFM). As shown in Figure 4a, the major peak at $d = 1.61$ nm in the X-ray diffraction pattern corresponds to the long axis of the molecule, which suggests that the molecules oriented normal to the substrate surface with certain extent of tilt. The tilt angle in thin film (estimated using the model presented in the Supporting Information) is significantly smaller than that in the single crystal. Though the exact molecular arrangement of the thin film is unclear yet, such a decrease

in the tilting angle has been proven to be beneficial to charge transport.¹² Higher-order diffraction peaks were clearly observed, showing good layered structure in the thin film. As illustrated in Figure 4b, AFM images showed that **1a** formed large, elongated grains. Such a thin film morphology is generally favorable for charge transport in FET.¹³

Similar performances were also observed from the FET devices using **1b** as the active material. Comparable hole mobility up to $0.4 \text{ cm}^2 \text{ V}^{-1} \text{ s}^{-1}$ was obtained. This result shows that the introduction of longer alkyl chains does not interfere with its OFET performance. Synthesis of molecules with the same core decorated with even longer alkyl chains is underway, to further investigate the effect of the side groups on device performance, and to develop solution-processable small molecule OFETs.

In conclusion, we have successfully realized high mobility OFET devices from a new thiophene containing heteroarenes. Top-contact FET devices were fabricated from **1a** and **1b** with hole mobility up to $0.4 \text{ cm}^2 \text{ V}^{-1} \text{ s}^{-1}$. These findings suggest that in addition to the much-explored linear acenes, molecules with a nonlinearly fused core could also be used as active materials in high-performance OFET. We are currently synthesizing heteroarenes with larger central cores, which might show better orbital overlap and device performance. Meanwhile, solution-processed devices using this series of molecules are under investigation and will be reported in due course.

Acknowledgment. This work was financially supported by the Major State Basic Research Development Program (2006CB921602 and 2007CB808000) and by the National Natural Science Foundation of China (NSFC).

Supporting Information Available: Detailed experimental procedures and characterization data of all new compounds (PDF). This material is available free of charge via the Internet at <http://pubs.acs.org>.

(11) Gruhn, N. E.; da Silva Filho, D. A.; Bill, T. G.; Malagoli, M.; Coropceanu, V.; Kahn, A.; Brédas, J.-L. *J. Am. Chem. Soc.* **2002**, *124*, 7918.

(12) Mannsfeld, S. C. B.; Virkar, A.; Reese, C.; Toney, M. F.; Bao, Z. *Adv. Mater.* **2009**, ASAP.

(13) Coropceanu, V.; Cornil, J.; da Silva Filho, D. A.; Olivier, Y.; Silbey, R.; Brédas, J.-L. *Chem. Rev.* **2007**, *107*, 926.